ARTICLE

BIOTECHNOLOGY and BIOENGINEERING

Surface Display of MPH on *Pseudomonas putida* JS444 Using Ice Nucleation Protein and Its Application in Detoxification of Organophosphates

Chao Yang,[1,2] Ning Cai,[1,2] Ming Dong,[3] Hong Jiang,[1] Jinming Li,[4] Chuanling Qiao,[1] Ashok Mulchandani,[5] Wilfred Chen[5]

[1]State Key Laboratory of Integrated Management of Pest Insects & Rodents, Institute of Zoology, Chinese Academy of Sciences, Beijing 100080, China; telephone: +86-10-6255-3369; fax: +86-10-6256-5689; e-mail: qiaocl@ioz.ac.cn

[2]Graduate School of the Chinese Academy of Sciences, Beijing, China

[3]Guangdong Poison Control Center, Guangzhou, China

[4]Tianjin Environmental Protection Bureau, Tianjin, China

[5]Department of Chemical and Environmental Engineering, University of California, Riverside, California 92521; telephone: 951-827-6419; fax: 951-827-5696; e-mail: adani@engr.ucr.edu

Received 13 March 2007; revision received 19 May 2007; accepted 29 May 2007

Published online 15 June 2007 in Wiley InterScience (www.interscience.wiley.com). DOI 10.1002/bit.21535

ABSTRACT: Methyl parathion hydrolase (MPH) has been displayed on the surface of microorganisms for the first time using only N- and C-terminal domains of the ice nucleation protein (INPNC) from *Pseudomonas syringae* INA5 as an anchoring motif. A shuttle vector pINCM coding for INPNC–MPH was constructed and used to target MPH onto the surface of a natural *p*-nitrophenol (PNP) degrader, *Pseudomonas putida* JS444, overcoming the potential substrate uptake limitation. Over 90% of the MPH activity was located on the cell surface as determined by protease accessibility and cell fractionation experiments. The surface localization of the INPNC–MPH fusion was further verified by Western blot analysis and immunofluorescence microscopy. The engineered *P. putida* JS444 degraded organophosphates as well as PNP rapidly without growth inhibition. Compared to organophosphorus hydrolase-displaying systems reported, changes in substrate specificity highlight an important potential use of the engineered strain for the clean-up of specific organophosphate nerve agents.

Biotechnol. Bioeng. 2008;99: 30–37.

KEYWORDS: organophosphate detoxification; methyl parathion hydrolase; surface display; ice nucleation protein; whole-cell biocatalyst

Introduction

Synthetic organophosphates (OPs) are widely used worldwide to control agricultural and household pests. Overall, OP compounds account for ~38% of total pesticides used globally (Singh and Walker, 2006). In the USA alone, over 40 million kilograms of organophosphorus pesticides are consumed annually (Shimazu et al., 2001b). These compounds have been implicated in several nerve and muscular diseases in human beings. OP poisoning is a worldwide health problem with around 3 million poisonings and 200,000 deaths annually (Karalliedde and Senanayake, 1999).

Bacterial enzymatic detoxification of OPs has attracted considerable interest, because it is economical and effective. Organophosphorus hydrolase (OPH), which is capable of hydrolyzing a wide range of oxon and thion OPs, has been extensively studied (Dumas et al., 1989; Mulbry and Karns, 1988). In the case of whole cells, the outer membrane acting as a permeability barrier prevents OPs from interacting with OPH residing within the cell (Richins et al., 1997). This bottleneck, however, could be eliminated if OPH is displayed onto the surface of cells. Recently, OPH was functionally expressed onto the cell surface using various anchoring strategies (Lei et al., 2005; Richins et al., 1997; Shimazu et al., 2001a,b).

Correspondence to: C. Qiao and A. Mulchandani

Contract grant sponsor: Innovation Program of the Chinese Academy of Sciences
Contract grant number: KSCX2-YW-G-008
Contract grant sponsor: Hi-Tech Research and Development Program of the People's Republic of China
Contract grant number: 2005AA601020

Gram-negative bacteria have developed various surface display systems for targeting foreign proteins on the cell surface with a wide range of applications (Lee et al., 2003; Samuelson et al., 2002). The ice nucleation protein (INP), an outer membrane protein from *P. syringae*, has been successfully used to display several proteins, such as levansucrase (Jung et al., 1998), salmobin (Jeong et al., 2001), green fluorescent protein (GFP) (Li et al., 2004), chitinase (Wu et al., 2006), and NADPH-cytochrome P450 oxidoreductase (Yim et al., 2006), on the surface of *Escherichia coli*. The INP, which nucleates ice formation in supercooled water (Wolber et al., 1986), has a multi-domain organization with an N-terminal domain containing three or four transmembrane spans, a C-terminal domain, and a highly repetitive central domain for ice nucleation (Kozloff et al., 1991; Wolber, 1993). It has been demonstrated that truncated INP derivatives containing N- and C-terminal domains (Shimazu et al., 2001a) or only N-terminal domain (Li et al., 2004) serve as anchoring motifs to target foreign proteins onto the cell surface of *E. coli*.

PNP, produced from hydrolysis of *p*-nitrophenyl-substituted OP compounds, is toxic to humans and has been listed as a priority pollutant by the USEPA (Lei et al., 2005). Co-inoculation of two engineered strains harboring *opd* gene and the genes for PNP mineralization has been shown to function cooperatively to remediate parathion-contaminated soils (Gilbert et al., 2003). PNP mineralizing *Moraxella* sp. and *Pseudomonas putida* JS444 were genetically engineered to complete mineralization of OP compounds by expressing OPH on the cell surface (Lei et al., 2005; Shimazu et al., 2001b).

Although OPH hydrolyzes a variety of OP neurotoxins, the rates vary from hydrolysis at the diffusion-controlled limit for paraoxon to several orders of magnitude slower for chlorpyrifos (Cho et al., 2004; Dumas et al., 1989). Recently, an OP degrading gene (called *mpd*) was isolated from a methyl parathion-degrading *Plesiomonas* sp., but showed no homology to the known *opd* genes (Cui et al., 2001). The highest similarity with predicted protein sequence was found to be 31% with β-lactamase, suggesting significant novelty of the gene–enzyme system.

We previously cloned *mpd* gene (GenBank accession number DQ677027) from a chlorpyrifos-degrading bacterium and the *mpd* gene was expressed in *E. coli* (Yang et al., 2006). Recombinant MPH with C-terminal His-tag showed high hydrolytic activities for various OPs. Practical applications of MPH in detoxification of OPs have been limited by the cost of purification and stability of the enzyme. Since OPs cannot easily diffuse across the outer membrane, the degradation of OPs by whole cells expressing intracellular MPH is very inefficient. To overcome the problems, an alternative strategy is the use of displayed MPH in detoxification of OPs.

In this work, we demonstrated that MPH could be successfully targeted onto the surface of *P. putida* JS444 using only N- and C-terminal domains of InaV (Schmid et al., 1997). Due to the altered specificity of MPH, the engineered strain is capable of rapidly degrading specific OP nerve agents such as chlorpyrifos compared to engineered strains with surface-expressed OPH.

Materials and Methods

Bacterial Strains and Plasmids

P. putida JS444 isolated from activated sludge by selective enrichment with PNP (Nishino and Spain, 1993) was used as a host for surface display of INPNC–MPH fusion. *E. coli* DH5α was selected as a control for displaying MPH. Plasmid pPNCO33 (Shimazu et al., 2001b), which contains only N- and C-terminal domains of the whole *inaV* gene (GenBank accession number AJ001086), was used to construct a surface expression vector. Plasmid pVLT33 (de Lorenzo et al., 1993) was used as a negative control in localization assays. Plasmid pMDQ (Yang et al., 2006) was used as the source of the *mpd* gene.

Construction of INPNC–MPH Fusion

For construction of gene fusion between INPNC and mature MPH, the regions encoding MPH without signal sequence were PCR amplified from plasmid pMDQ with forward primer 5′-ACGGATCCCGGGATGGCCGCACCGCAGGT-GCGCACCTCG-3′ and reverse primer 5'-GTAAGCTT-CACTTGGGGTTGACGACCG-3′ (the *Bam*HI and *Hin*dIII sites, respectively, are underlined). PCR products were digested with *Bam*HI and *Hin*dIII and inserted into similarly digested pPNCO33 to generate pINCM. pINCM directs the expression of fusion which contains the N- and C-terminal domains of InaV and mature MPH with the initiator, methionine. Expression of INPNC–MPH was under the control of a tightly regulated *tac* promoter.

To generate pCPM for expressing MPH in the cytoplasm, the amplified *mpd* gene was digested with *Eco*RI and *Hin*dIII and inserted into a similarly digested pPNCO33. PCR amplification of *mpd* gene was the same as the above PCR except for forward primer 5′-ACGAATTCAGGAAA-CAATGGCCGCACCGCAGGTGCGC-3′ (the *Eco*RI site is underlined).

Transformation of plasmid into *P. putida* JS444 or *E. coli* DH5α was performed using the $MgCl_2$ or $CaCl_2$ method (Sambrook and Russel, 2001; Shimazu et al., 2003). Expression of INPNC–MPH was induced with 1 mM IPTG for 24 h at 30°C when cells were grown to an $OD_{600} = 0.4$.

Western Blot Analysis

After *P. putida* JS444 and *E. coli* DH5α cells expressing INPNC–MPH fusion were harvested, cell fractionation was performed according to the method described in Lei et al. (2005). Samples of total cell lysate, soluble fraction, and membrane fraction were analyzed on SDS-PAGE with 10% (w/v) acrylamide (Sambrook and Russel, 2001) and electrophoretically transferred onto a nitrocellulose membrane

with a tank transfer system. After blocking non-specific binding sites with 3% BSA in TBST solution, the membrane was incubated with rabbit anti-INPNC polyclonal serum (Kwak et al., 1999) at a 1:1,000 dilution at 30°C for 2 h and washed with TBST. Subsequently, the membrane was allowed to react with alkaline phosphatase-conjugated goat anti-rabbit IgG antibody (Promega, Madison, WI) at a 1:1,000 dilution at 30°C for 1 h. The membrane was then stained with NBT/BCIP (Novagen, Darmstadt, Germany) for visualizing antigen-antibody conjugates.

Immunofluorescence Microscopy

P. putida JS444 cells were harvested and washed with PBS buffer (pH 7.4), and then resuspended in PBS containing 3% BSA ($OD_{600} = 0.5$) for blocking at 30°C for 1 h. After blocking with PBS + BSA solution, cells were incubated with rabbit anti-INPNC serum (Kwak et al., 1999) diluted (1:1,000) in PBS + BSA solution at 30°C for 2 h, and then washed five times with PBS. After washing with PBS buffer, the cell-antibody complex was incubated with goat anti-rabbit IgG conjugated with TRITC (Invitrogen, Mukilteo, WA) at a dilution of 1:1,000 at 30°C for 1 h. Finally, cells were washed five times with PBS and observed by a fluorescence microscope (Olympus, Tokyo, Japan).

MPH Activity Assay

P. putida JS444 cells harboring pINCM or pCPM were grown, harvested, and resuspended in 100 mM phosphate buffer (pH 7.4). Cell lysate was prepared by addition of 10 μL of lysozyme (10 mg/mL) and incubated on ice for 1 h, followed by sonication in three pulses of 10 s each. MPH activity assay mixtures (1 mL, 3% methanol) contained 50 μg/mL methyl parathion (added from a 10 mg/mL methanol stock solution), 960 μL of 100 mM phosphate buffer (pH 7.4), and 10 μL of cells ($OD_{600} = 1.0$). Changes in absorbance (405 nm) were measured for 3 min at 30°C. Activities were expressed as units (1 μmol of PNP formed per minute) per milligram of protein ($\varepsilon_{405} = 17{,}700\ M^{-1}\ cm^{-1}$ for PNP). Similar whole-cell activity measurements were conducted with *E. coli* DH5α harboring pINCM.

Proteinase Accessibility Assay

P. putida JS444 cells harboring pINCM or pCPM were centrifuged and resuspended in 1 mL of 15% sucrose, 15 mM Tris–HC1, and 0.1 mM EDTA, pH 7.8. Samples were incubated for 1 h with 5 μL of 20 mg/mL proteinase K at room temperature. To inhibit further proteinase K activity, 10 μM phenylmethylsulfonylfluoride was added after incubation. Proteinase K-treated and untreated cells were assayed for MPH activity as described above.

Detoxification of Organophosphates by the Engineered *P. putida* JS444

For the organophosphorus pesticides and PNP degradation experiments, *P. putida* JS444 carrying pINCM was inoculated at an $OD_{600} = 0.1$ in minimal salts medium (Spain and Nishino, 1987) supplemented with 1 mM IPTG, 0.2 mM PNP, 0.1% yeast extract, and 50 μg/mL kanamycin and incubated at 30°C and 300 rpm until the yellow color of PNP disappeared. The cells were centrifuged at 4°C, followed by washing with 100 mM phosphate buffer (pH 7.4), and resuspended in the same buffer. Then, cell suspensions ($OD_{600} = 0.4$) were incubated with 0.4 mM parathion, methyl parathion, fenitrothion, or chlorpyrifos. The pesticide residues were measured by GC-ECD (Yang et al., 2006).

Whole Cell Activity of *P. putida* JS444 Containing pPNCO33 or pINCM

Using four different substrates, OPH- and MPH-displaying *P. putida* JS444 strains were measured for whole cell activity. The rates of parathion and methyl parathion hydrolysis were measured spectrophotometrically by monitoring the production of PNP at 405 nm. The rate of fenitrothion hydrolysis was measured by monitoring the formation of MNP at 358 nm ($\varepsilon_{358} = 18{,}700\ M^{-1}\ cm^{-1}$) (Dumas et al., 1989). The rate of chlorpyrifos hydrolysis was measured by HPLC (Yang et al., 2006). The standard assay for the enzyme activity was carried out in 100 mM phosphate buffer (pH 7.4) and 0.2 mM substrate at 30°C. Activities were expressed as units (1 μmol of substrate hydrolyzed per minute) per milligram of protein.

Results

Surface Display of INPNC–MPH

To investigate the feasibility of targeting MPH onto the surface of *P. putida* JS444, the truncated InaV (INPNC) from *P. syringae* INA5 was used as the surface anchor. Plasmid pINCM, carrying the *inpnc–mpd* fusion was constructed by inserting the *mpd* fragment into an *E. coli*/*Pseudomonas* shuttle vector, pPNCO33. Expression of the INPNC–MPH fusion was under the control of a tightly regulated *tac* promoter.

The percentage of MPH on the cell surface was estimated by measuring MPH activity in the membrane and soluble cell fractions. Over 90% of the activity was detected in the membrane fractions (Table I). In parallel, more than 90% of MPH activity was present on the cell surface as judged from the activity ratio between whole cells (10.72 U/mg protein) and cell lysates (11.53 U/mg protein). Finally, protease accessibility experiments were performed to ascertain the surface localization of MPH. Cells were incubated with proteinase K in the presence of EDTA. Since proteinase K cannot readily diffuse across the cell membrane, degradation should only occur with proteins exposed on the surface. After 1 h of incubation, the MPH activity for cells carrying pINCM decreased by 83%, while cells expressing MPH

DOI 10.1002/bit

Table I. Percentage of surface-exposed MPH as estimated from proteinase K treatment, whole cell versus lysate assays, and membrane fractionation experiments; experiments conducted with *P. putida* JS444 carrying either pINCM or pCPM.

Plasmid	% Decrease in activity in proteinase K treated cells	Whole-cell activity (as % of lysate activity)	% Activity in membrane fraction
pINCM	83	91	93
pCMP	6	2	5

intracellularly (pCPM) had only a 6% drop in activity (Table I).

To verify the synthesis of INPNC–MPH fusion, Western blot was performed with whole-cell lysates of *P. putida* JS444 carrying pINCM or pVLT33 after induction with 1 mM IPTG. INPNC–MPH fusion was observed from cells carrying pINCM at the position of ca. 68 kDa, which matched well with the molecular mass estimated from the deduced amino acid sequence of the fusion (Fig. 1A). However, no such protein was detected with the control cells carrying pVLT33. To assess the distribution of the fusion between the membrane and soluble fractions, total cell lysate, membrane, and soluble fractions were probed with anti-INPNC serum. As shown in Figure 1A, more than 90% of the fusion was associated with the membrane fraction as judged by the intensity of the protein band. To investigate the effect of host strains on the efficiency of surface expression, Western blot was also performed with *E. coli* DH5α harboring pINCM. Only 20% of the fusion was associated with the membrane fraction of *E. coli* DH5α (Fig. 1B), consistent with the activity distribution between the membrane (2.38 U/mg protein) and soluble fractions (9.89 U/mg protein).

To investigate whether INPNC–MPH fusion was displayed correctly on *P. putida* surface in a stable conformation, immunofluorescence microscopy was used. Cells were probed with rabbit anti-INPNC serum as a primary antibody and then fluorescently stained with TRITC-labeled goat anti-rabbit IgG antibody. Under the immunofluorescence microscopy, the orange fluorescence was observed on the cells harboring pINCM (Fig. 2B). In contrast, the control cells harboring pVLT33 were not immunostained (Fig. 2A). These results indicated that the cell surface of *P. putida* was covered with antibody-TRITC complex, which confirmed that INPNC–MPH fusion was successfully displayed on the surface of *P. putida*.

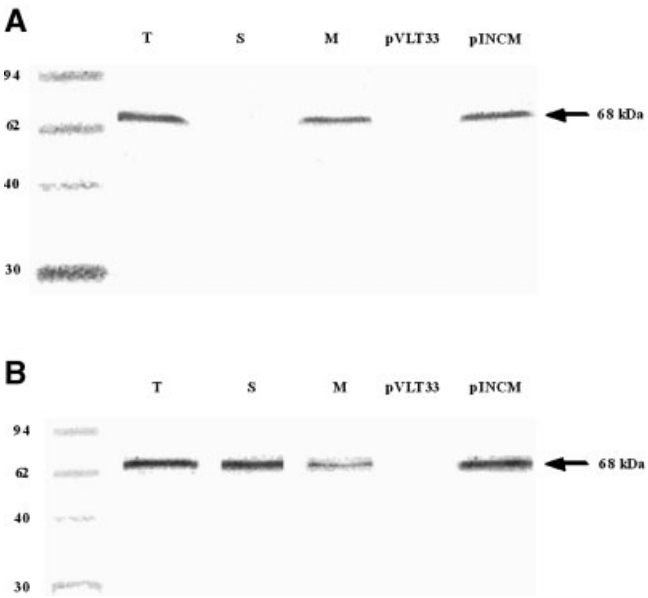

Figure 1. Western blot analysis for subcellular location of expressed INPNC–MPH fusion in *P. putida* JS444 (**A**) and *E. coli* DH5α (**B**) harboring pINCM. The amount of INPNC–MPH in total cell lysate (T), soluble fraction (S), and membrane fraction (M) was detected with rabbit anti-INPNC serum at a 1:1,000 dilution. Arrow indicates the location of the fusion. Cells harboring pVLT33 were used as a negative control.

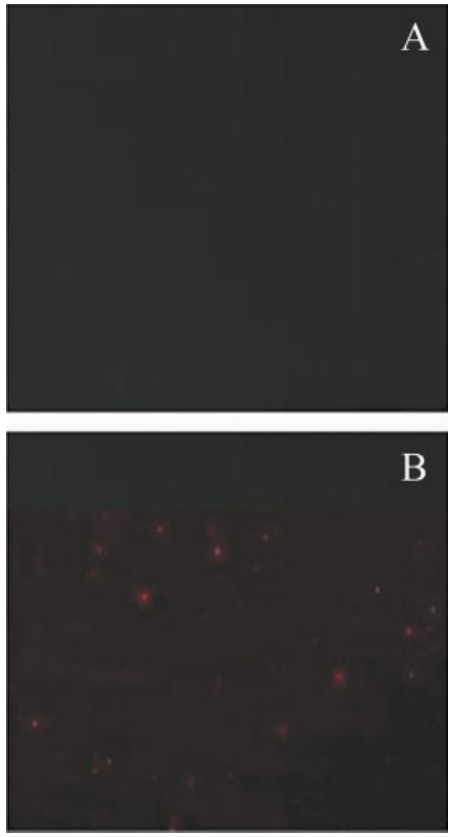

Figure 2. Immunofluorescence micrographs of *P. putida* JS444 harboring pVLT33 (**A**) and pINCM (**B**). Cells were probed with rabbit anti-INPNC serum and fluorescently stained with goat anti-rabbit IgG-TRITC conjugate. [Color figure can be seen in the online version of this article, available at www.interscience.wiley.com.]

Catalytic Activities

The whole-cell activities of recombinant *P. putida* JS444 displaying MPH were 40-fold higher than those of the same strain expressing MPH in the cytoplasm when using the same amount of cells (Fig. 3). Moreover, *P. putida* JS444 harboring pINCM exhibited 10-fold higher activity than *E. coli* DH5α harboring the same plasmid (Fig. 3). Time course analysis of the activity of MPH-displaying cells indicated that the highest activity of whole cells appeared at 24 h after induction with 1 mM IPTG (Fig. 4). However, the activity in total cell lysate reached a maximum at 12 h and remained constant thereafter. To investigate the optimal conditions for cell surface-displayed MPH, whole-cell MPH activities of *P. putida* JS444 harboring pINCM were measured at different temperatures (20–40°C) and at pH 6–10. The maximum activity of cell surface-displayed MPH was observed at 30°C and pH 8.0. In the temperature range from 25 to 35°C and in the pH range from 7 to 9, the whole-cell activities were more than 90% of the maximum activity. Enzymatic characteristics of His-tagged MPH have been determined (unpublished work). The pH and temperature profiles of surface-displayed MPH are similar to those of His-tagged MPH.

Detoxification of Organophosphates by the Engineered *P. putida* JS444

As shown in Figure 5A, methyl parathion was quickly degraded within the first 30 min with almost stoichiometric release of PNP. Both 0.4 mM PNP and methyl parathion were completely mineralized in 5 h. Display of MPH on *P. putida* JS444 surface had no effect on PNP degradation; recombinant strains degraded PNP at the same rate as wild-type *P. putida* JS444. Complete hydrolysis of parathion and fenitrothion occurred within 150 and 80 min, respectively (Fig. 5B and C). This decrease in hydrolysis rate is consistent with the kinetic properties of MPH, which is more efficient in hydrolyzing methyl parathion than other organophosphorus pesticides (Fu et al., 2004). The PNP produced from

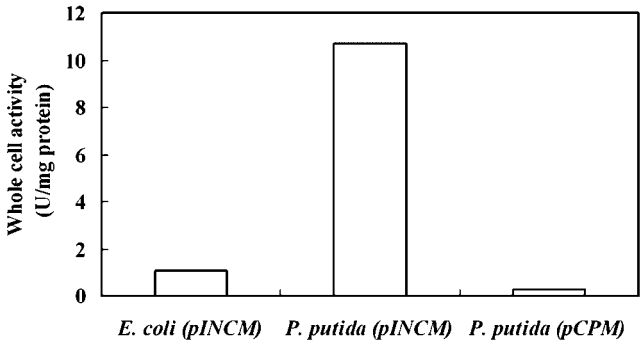

Figure 3. Whole-cell MPH activities of *E. coli* DH5α (pINCM) and *P. putida* JS444 (pINCM or pCPM).

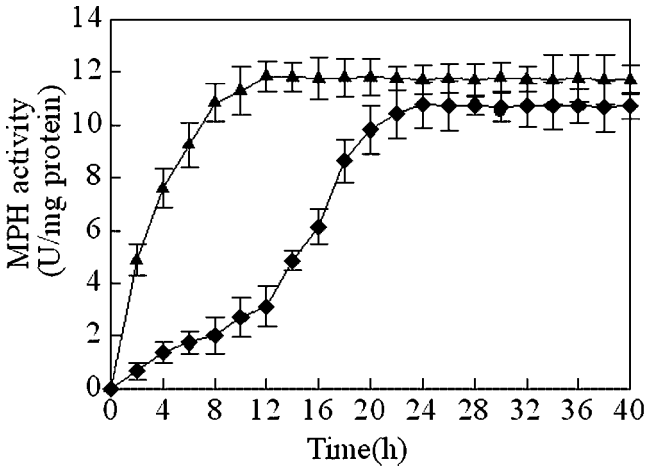

Figure 4. Time course analysis of the activity of MPH-displaying cells. *P. putida* JS444 cells were incubated at 30°C for 40 h after induction with 1 mM IPTG. The activity of whole cell (◆) and total cell lysate (▲) was determined as described in Materials and Methods. The data are the mean ± SD for three independent experiments.

hydrolysis of parathion was completely degraded within 5 h (Fig. 5B). OPH has almost no hydrolytic activity for chlorpyrifos (~1,200-fold less efficient than paraoxon) (Cho et al., 2004). Recombinant *P. putida* JS444 displaying MPH hydrolyzed 0.4 mM chlorpyrifos within 200 min (Fig. 5D).

Comparative Study of OPH- and MPH-displaying *P. putida* JS444 Cells

As shown in Figure 6, *P. putida* JS444 cells with surface-displayed MPH showed higher activity for dimethyl OPs such as methyl parathion and fenitrothion than OPH-displaying cells. There was a slight drop in activity for parathion observed with MPH-displaying cells. *P. putida* JS444 cells displaying MPH showed high activity for chlorpyrifos, but only very low activity was detected with OPH-displaying cells. These results highlight an important potential use of the engineered strain for the clean-up of specific OP nerve agents compared to OPH-displaying systems reported (Lei et al., 2005; Shimazu et al., 2001b).

Discussion

Most cell-surface display systems are limited in the size of foreign protein that can be expressed (Samuelson et al., 2002). The INP-based anchoring systems from genus *Pseudomonas* can express larger proteins, such as 77 kDa CPR (Yim et al., 2006), and 90 kDa Chi92 (Wu et al., 2006). The two types of the several identified INPs that have been used widely for display of foreign proteins on the cell surface are InaK from *P. syringae* KCTC 1832 (Jung et al., 1998) and InaV from *P. syringae* INA5 (Schmid et al., 1997). Even though functionally similar, there is only 77% sequence

DOI 10.1002/bit

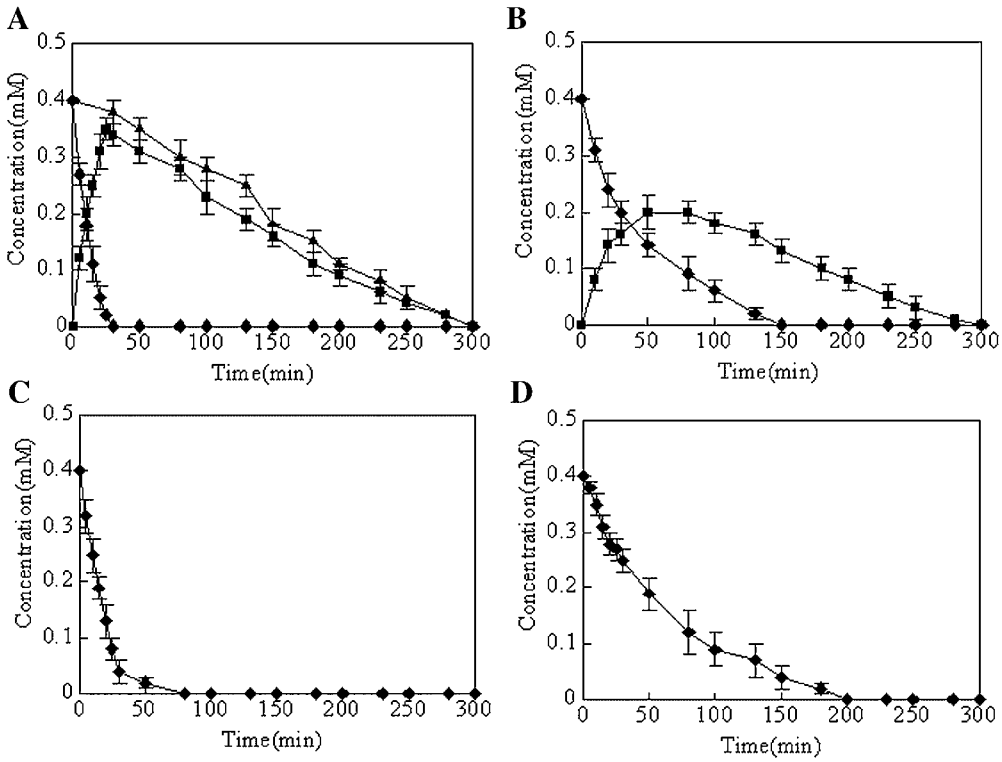

Figure 5. Detoxification of organophosphates by *P. putida* JS444 harboring pINCM. **A**: Methyl parathion, (**B**) parathion, (**C**) fenitrothion, and (**D**) chlorpyrifos. All substrates were added at 0.4 mM. Symbols: (◆) organophosphorus pesticides; (■) PNP formed during the hydrolysis of OPs; (▲) degradation of 0.4 mM PNP by *P. putida* JS444 harboring pINCM. The data are the mean ± SD for three independent experiments.

homology between the two proteins. Most of the differences occur at the critical N-terminal domain, which interacts with the phospholipids moiety of the outer membrane (Kozloff et al., 1991; Wolber, 1993). Compared to InaK anchor, the use of InaV anchor resulted in 5- and 100-fold higher OPH activity in *E. coli* and *Moraxella* sp., respectively (Shimazu et al., 2001a,b). We previously displayed CaE B1 (60 kDa) on *E. coli* surface using the InaV anchor (Zhang et al., 2004). The aim of this study was to explore the feasibility of targeting MPH onto the cell surface using the InaV anchor. A shuttle vector, pINCM, coding for INPNC–MPH was constructed and the surface localization and functionality of MPH were demonstrated in *P. putida* JS444. The physical binding between MPH and OP was reinforced by expressing MPH on *P. putida* surface and it assists the catalytic activity of this enzyme.

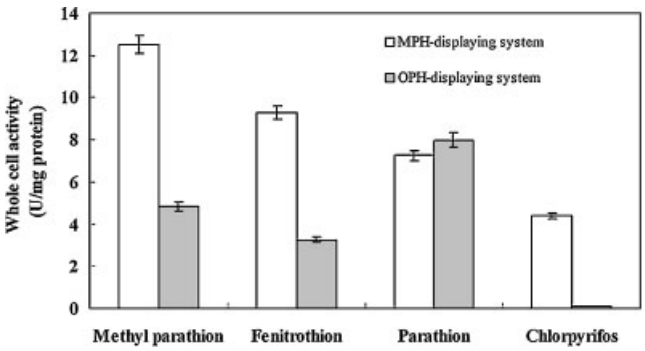

Figure 6. Whole cell activity of *P. putida* JS444 containing pINCM or pPNCO33.

Time course of whole-cell activity suggests that stationary-phase translocation of previously synthesized INPNC–MPH fusion may be responsible for the improved whole-cell activity (Fig. 4). A similar observation has been reported for the surface expression of OPH using the INP anchor (Shimazu et al., 2001b). In the context of expression and secretion of a protein, secretion is generally the limiting step; thus, a high transcription rate can block the translocation pathway and cause growth inhibition (Shi and Su, 2001). When using the N-terminal domain of InaK as an anchoring motif, growth inhibition was observed in GFP- and Chi92-displaying cells under 1 mM IPTG induction (Li et al., 2004; Wu et al., 2006). To test whether the high-level expression of INPNC–MPH inhibits cell growth, growth kinetics of *P. putida* JS444 cells carrying pINCM or pVLT33 were compared. No growth inhibition was observed for cells expressing INPNC–MPH. The *P. putida* JS444/pINCM showed the same growth profile as JS444/pVLT33 (data not shown).

Cell surface display in *Pseudomonas* has not been studied extensively in spite of the high biocatalytic potential of

Pseudomonas displaying enzymes. Whole-cell MPH activity of recombinant *P. putida* JS444 was 10-fold greater than that of *E. coli* DH5α using the INP anchor. The improved activity observed here is in line with previous report using the INP anchor for the surface expression of OPH in *P. putida* KT2440 (Shimazu et al., 2003). This increase in surface targeting of MPH/OPH in *P. putida* could be due to improved membrane translocation since the INP anchor originated from *Pseudomonas* strains. Therefore, this remarkably high level of surface expression could potentially be utilized for the display of a wide range of peptides and enzymes onto the surface of *P. putida*.

Although MPH is similar to OPH in substrate range, it is still different from OPH in other aspects. The *mpd* and *opd* genes appear to have evolved from different sources; they have little sequence similarity. MPH belongs to the metallo-β-lactamase superfamily, while OPH belongs to the phosphotriesterase family. MPH is a monomer, while OPH is a dimmer. There are 71 commercial organophosphorus pesticides listed in Tomlin (2003), of which 33 and 26, respectively, contain diethyl and dimethyl alkyl groups. OPH has already been shown to lack any hydrolytic activity towards numerous dimethyl OPs (Horne et al., 2002). Changes in substrate specificity have been reported for MPH, which exhibits higher k_{cat}/K_m values for dimethyl OPs such as methyl parathion (Fu et al., 2004). Therefore, *P. putida* JS444 with surface-expressed MPH may be a potential candidate at low cost for the remediation of pollution caused by dimethyl OPs.

P. putida JS444, isolated from PNP-contaminated waste sites, is particularly attractive as it can rapidly degrade PNP (Nishino and Spain, 1993). In this work, a surface expression vector pINCM allowed the expression of a sufficient quantity of MPH onto the cell surface of *P. putida* JS444, resulting in strains with both OP degradation and PNP mineralization capabilities. Moreover, the surface-displayed MPH retained high hydrolytic activity and had similar enzymatic characteristics to native MPH. Functional expression of MPH on the surface of microbes is demonstrated and suggests that it can be a potential whole-cell biocatalyst for the remediation of highly toxic OP nerve agents.

Conclusion

To date, there are no reports of the surface expression of MPH on the surface of microorganisms. In this work, MPH was successfully displayed on the cell surface of a natural PNP degrader, *P. putida* JS444, using a functional truncated INP motif. The engineered strain degraded OPs as well as PNP rapidly without growth inhibition. Compared to recombinant *P. putida* JS444 displaying OPH (Lei et al., 2005), the engineered strain displaying MPH showed high activity for specific substrates such as chlorpyrifos, which makes it a novel biocatalyst for the remediation of pollution caused by specific OP nerve agents.

This work was supported by grants from the Innovation Program of the Chinese Academy of Sciences (No. KSCX2-YW-G-008) and the 863 Hi-Tech Research and Development Program of the People's Republic of China (No. 2005AA601020).

References

Cho CM, Mulchandani A, Chen W. 2004. Altering the substrate specificity of organophosphorus hydrolase for enhanced hydrolysis of chlorpyrifos. Appl Environ Microbiol 70:4681–4685.

Cui ZL, Li SP, Fu GP. 2001. Isolation of methyl parathion-degrading strain M6 and cloning of the methyl parathion hydrolase gene. Appl Environ Microbiol 67:4922–4925.

de Lorenzo V, Eltis L, Kessler B, Timmis KN. 1993. Analysis of *Pseudomonas* gene using *lacI*^{q}/P*trp-lac* plasmids and transposons that confer conditional phenotypes. Gene 123:17–24.

Dumas DP, Caldwell SR, Wild JR, Raushel FM. 1989. Purification and properties of the phosphotriesterase from *Pseudomonas diminuta*. J Biol Chem 264:19659–19665.

Fu GP, Cui ZL, Xu W, Wu XP, Li SP. 2004. Recombinant expression of methyl parathion hydrolase gene and its purification and characterization. Acta Microbiol Sin 44:356–360.

Gilbert ES, Walker AW, Keasling JD. 2003. A constructed microbial consortium for biodegradation of the organophosphorus insecticide parathion. Appl Microbiol Biotechnol 61:77–81.

Horne I, Sutherland TD, Harcourt RL, Russell RJ, Oakeshott JG. 2002. Identification of an *opd* (organophosphate degradation) gene in an *Agrobacterium* isolate. Appl Environ Microbiol 68:3371–3376.

Jeong HS, Yoo SK, Kim EJ. 2001. Cell surface display of salmobin, a thrombin-like enzyme from *Agkistrodon halys* venom on *Escherichia coli* using ice nucleation protein. Enzyme Microb Technol 28:155–160.

Jung HC, Lebeault JM, Pan JG. 1998. Surface display of *Zymomonas mobilis* levansucrase by using the ice-nucleation protein of *Pseudomonas syringae*. Nat Biotechnol 16:576–580.

Karalliedde L, Senanayake N. 1999. Organophosphorus insecticide poisoning. J Int Fed Clin Chem 11:4–9.

Kozloff LM, Turner MA, Arellano F. 1991. Formation of bacterial membrane ice-nucleation lipoglycoprotein complexes. J Bacteriol 173:6528–6536.

Kwak YD, Yoo SK, Kim EJ. 1999. Cell surface display of human immunodeficiency virus type 1 gp120 on *Escherichia coli* by using ice nucleation protein. Clin Diagn Lab Immunol 6:499–503.

Lee SY, Jong HC, Zhaohui X. 2003. Microbial cell-surface display. Trends Biotechnol 21:45–52.

Lei Y, Mulchandani A, Chen W. 2005. Improved degradation of organophosphorus nerve agents and *p*-nitrophenol by *Pseudomonas putida* JS444 with surface-expressed organophosphorus hydrolase. Biotechnol Prog 21:678–681.

Li L, Kang DG, Cha HJ. 2004. Functional display of foreign protein on surface of *Escherichia coli* using N-terminal domain of ice nucleation protein. Biotechnol Bioeng 85:214–221.

Mulbry WW, Karns JS. 1988. Parathion hydrolase specified by the *Flavobacterium opd* gene: Relationship between the gene and protein. J Bacteriol 171:6740–6746.

Nishino SF, Spain JC. 1993. Cell density-dependent adaption of *Pseudomonas putida* to biodegradation of *p*-nitrophenol. Environ Sci Technol 27:489–493.

Richins RD, Kaneva I, Mulchandani A, Chen W. 1997. Biodegradation of organophosphorus pesticides by surface-expressed organophosphorus hydrolase. Nat Biotechnol 15:984–987.

Sambrook J, Russel DW. 2001. Molecular Cloning: A laboratory manual, 3rd edn. Cold Spring Harbor, NY: Cold Spring Harbor Laboratory Press.

Samuelson P, Gunneriusson E, Nygren PA, Stahl S. 2002. Display of proteins on bacteria. J Biotechnol 96:129–154.

DOI 10.1002/bit

Schmid D, Pridmore D, Capitani G, Battistuta R, Nesser JR, Jann A. 1997. Molecular organization of the ice nucleation protein InaV from *Pseudomonas syringae*. FEBS Lett 414:590–594.

Shi H, Su WW. 2001. Display of green fluorescent protein on *Escherichia coli* cell surface. Enzyme Microb Technol 28:25–34.

Shimazu M, Mulchandani A, Chen W. 2001a. Cell surface display of organophosphorus hydrolase using ice nucleation protein. Biotechnol Prog 17:76–80.

Shimazu M, Mulchandani A, Chen W. 2001b. Simultaneous degradation of organophosphorus pesticides and *p*-nitrophenol by a genetically engineered *Moraxella* sp. with surface-expressed organophosphorus hydrolase. Biotechnol Bioeng 76:318–324.

Shimazu M, Nuyen A, Mulchandani A, Chen W. 2003. Cell surface display of organophosphorus hydrolase in *Pseudomonas putida* using ice nucleation protein anchor. Biotechnol Prog 19:1612–1614.

Singh BK, Walker A. 2006. Microbial degradation of organophosphorus compounds. FEMS Microbiol Rev 30:428–471.

Spain JC, Nishino SF. 1987. Degradation of 1,4-dichlorobenzene by a *Pseudomonas* sp. Appl Environ Microbiol 53:1010–1019.

Tomlin C. 2003. The pesticide manual, 13th edn. Hampshire, UK: BCPC Publications.

Wolber PK. 1993. Bacterial ice nucleation. Adv Microb Physiol 34:203–237.

Wolber PK, Deininger CA, Southworth MW, Vandekerckhove J, van Montagu M, Warren GJ. 1986. Identification and purification of a bacterial ice-nucleation protein. Proc Natl Acad Sci USA 83:7256–7260.

Wu ML, Tsai CY, Chen TH. 2006. Cell surface display of Chi92 on *Escherichia coli* using ice nucleation protein for improved catalytic and antifungal activity. FEMS Microbiol Lett 256:119–125.

Yang C, Liu N, Guo XM, Qiao CL. 2006. Cloning of *mpd* gene from a chlorpyrifos-degrading bacterium and use of this strain in bioremediation of contaminated soil. FEMS Microbiol Lett 265:118–125.

Yim SK, Jung HC, Pan JG, Kang HS, Ahn T, Yun CH. 2006. Functional expression of mammalian NADPH-cytochrome P450 oxidoreductase on the cell surface of *Escherichia coli*. Protein Expr Purif 49:292–298.

Zhang JL, Lan WS, Qiao CL, Jiang H, Mulchandani A, Chen W. 2004. Bioremediation of organophosphorus pesticides by surface-expressed carboxylesterase from mosquito on *Escherichia coli*. Biotechnol Prog 20:1567–1571.